

Optical design of a broadband atmospheric dispersion corrector for MAVIS

Davide Greggio^{*a,b}, Christian Schwab^c, Demetrio Magrin^{a,b}, Simone Di Filippo^{a,b,d}, Valentina Viotto^{a,b}, François Rigaut^e

^a INAF – Osservatorio Astronomico di Padova, Vicolo dell'Osservatorio 5, 35122 Padova, Italy

^b ADONI – ADaptive Optics National laboratory in Italy

^c Australian Astronomical Optics – Macquarie University, 105 Delhi Rd, North Ryde NSW, 2113

^d Dipartimento di Fisica ed Astronomia G. Galilei – Università degli Studi di Padova, Vicolo dell'Osservatorio 3, 35122 Padova, Italy

^e The Australian National University, Mount Stromlo Observatory Weston ACT 2611

ABSTRACT

The MCAO Assisted Visible Imager and Spectrograph (MAVIS), is a new instrument for ESO's Very Large Telescope. The science instruments, namely an imager and a spectrograph observing at VIS wavelengths (370-1000nm), are fed by a MCAO module which performs wide field wavefront sensing and correction by means of both NGS and LGS stars. To maximize sky coverage, tip-tilt sensing is done at NIR wavelengths (1000-1700 nm) by selecting up to three stars in a 2arcmin FoV. In order to maximize the stability between NGS wavefront sensor and scientific instruments, we designed a common-path Atmospheric Dispersion Corrector (ADC) able to efficiently compensate for atmospheric differential refraction in the full wavelength range used by the MAVIS sub-systems.

In this paper we present the design of the ADC. A few possible combinations of glasses are proposed and compared in terms of residual chromatic aberration, throughput, exit pupil movement and total thickness of the prism assembly.

Keywords: MAVIS, atmospheric dispersion correction, atmospheric compensation, Amici prism, optical design, optimization, prisms, glasses

1. INTRODUCTION

To achieve diffraction-limited imaging at visible wavelengths at an 8-meter diameter ground-based telescope like the VLT, it is necessary to compensate for the effects of the atmosphere. Other than atmospheric turbulence, one of the results of the light passing through the Earth's atmosphere is differential atmospheric refraction. This manifests as a differential dispersion of wavelengths along the altitude direction, resulting in small spectra out of a broadband point source.

The amplitude of atmospheric dispersion depends on some environmental parameters, mainly temperature and pressure, but also relative humidity and CO₂ concentration. Moreover, atmospheric dispersion is greatly dependent on the zenith distance of observation, meaning that its amplitude changes with the altitude pointing of the telescope.

In order to correct for it, it is necessary to add an opposite dispersion that compensates for the atmospheric one. This is usually achieved by using low dispersion prisms producing a dispersion curve that closely matches that of the atmosphere. The compensating mechanism should also be able to adjust its dispersing power to adapt to the zenith distance of the observation and should avoid any other side effects like pupil and image motion.

While Atmospheric Dispersion Correctors (ADCs) have been widely used in astronomical instrumentation since many decades, the ever-increasing resolution and stability required by new instruments call for high-performing devices, able to achieve residual dispersions of a few tens of milliarcseconds PTV or better. In this paper, we present the optical design of the ADC designed for MAVIS^[1]. To limit NCPA aberrations and maximize stability, the ADC is placed in the common path between the science channel and the NGS wavefront sensor channel and needs to correct for atmospheric dispersion in the extremely wide wavelength range 370-1700nm.

*davide.greggio@inaf.it;

2. ATMOSPHERIC DISPERSION CORRECTOR DESIGN

The configuration adopted for the ADC of MAVIS is based on counter-rotating amici prisms^[2]. In this configuration, two identical Amici prisms (i.e. compound prisms with zero deviation at a given design wavelength), can rotate around the optical axis. When the dispersion axes of the two prisms are aligned, their dispersing power adds, while when they are positioned at 180° one with respect to the other, their dispersing power cancels out. By rotating in between these two extreme positions, it is possible to adapt the correction to different zenith distances.

Even if it is not a rule, in order to minimize aberrations on the transmitted wavefront, a counter-rotating prisms ADC should be placed in a collimated beam. Moreover, placing the two prisms next to a pupil plane prevents from generating lateral chromatic aberrations in the following images of the pupil.

The optical design of the adaptive optics module of MAVIS (AOM)^[3] provides a collimated beam in the NGS/Science common path and this is where the ADC has been placed. The ADC is not exactly at a pupil plane because it is not accessible, nonetheless the distance from the pupil image has been minimized as much as possible in order to limit lateral chromatic aberrations in the exit pupil when the ADC is correcting atmospheric dispersion. The beam diameter at the ADC location is 57.1mm, which corresponds to a de-magnification factor of 140 with respect to the VLT-UT4 entrance pupil. This means that the atmospheric angular dispersion is multiplied by the same amount at the ADC position.

2.1 Atmospheric dispersion profile

Since we are interested in differential refraction within a given wavelength range rather than absolute refraction (the latter can be compensated by telescope pointing), we can use the approximation provided by Smart^[4]. In this approximation, the differential angular dispersion $\Delta R(\lambda)$ depends only on the refractive index of air and on the zenith distance of observation:

$$\Delta R(\lambda) \approx 206265 \cdot \left(n(\lambda) - n(\lambda_{ref}) \right) \cdot \tan z \quad [arcsec]$$

The dependence on the tangent of the zenith angle z is an approximation valid up to approximately $z=60$ deg. Sometimes also a second term in the expansion is added, replacing the $\tan z$ with $(A \cdot \tan z + B \cdot \tan^2 z)$, where the coefficients A and B are calculated by best fitting of a model of the atmosphere. Here we used the simple $\tan z$ relationship.

Many models of air refractivity are available in the literature. We used the formulation by Ciddor^[5], who claims an error on the refractive index of air of about $2 - 5 \cdot 10^{-8}$ within the wavelength range 300-1690nm, corresponding to an error on differential dispersion of about 10-20 mas at a zenith distance of $z=65^\circ$. Figure 1 shows a comparison of different models from literature^[5-9] using the Ciddor model as reference. Note that the atmospheric dispersion model provided by the software Zemax OpticStudio, which is widely used in ADC design and optimization, underestimates the dispersion at short wavelengths by approximately 20mas if we consider observations at a zenith distance of 60° .

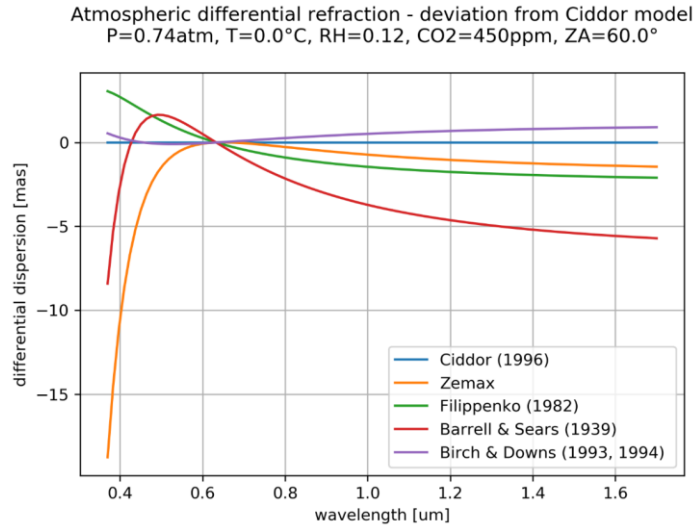


Figure 1. Comparison of different atmospheric dispersion models from literature (Ciddor model used as reference).

The reference wavelength is $\lambda_{ref} = 633nm$.

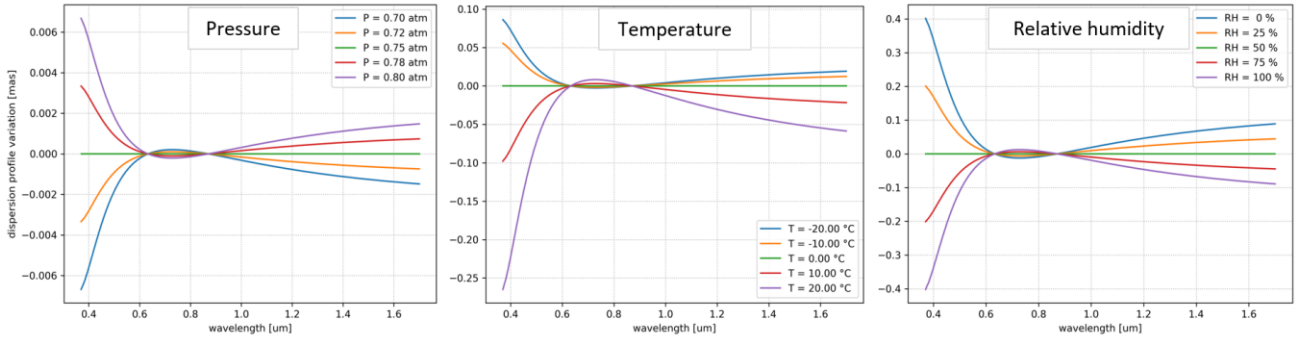


Figure 2. Variation of the atmospheric dispersion profile shape as a function of pressure (left), temperature (middle) and relative humidity (right). The reference profile used in the example (green curve) has $P=0.75atm$, $T=0.0^{\circ}C$ and $RH=50\%$.

In the Ciddor model, the refractivity of air is expressed as a function of the following atmospheric parameters: pressure, temperature, relative humidity and CO_2 concentration. The parameters that we assumed for our analysis are reported in Table 1. Even if a variation of the atmospheric parameters affects the total amount of dispersion, its impact on the relative dispersion between wavelengths is much smaller. This is shown in Figure 2, where we plot the variation of profile shape $\delta(\lambda)$, with respect to a reference atmospheric dispersion profile ($P=0.75atm$, $T=0.0^{\circ}C$ and $RH=50\%$), as a function of pressure (left), temperature (middle) and relative humidity (right). With variation of shape $\delta(\lambda)$ we mean that the new dispersion profile can be expressed as:

$$\Delta R(\lambda) = k \cdot \Delta R(\lambda)_{ref} + \delta(\lambda)$$

Where k is a multiplicative constant and $\Delta R(\lambda)_{ref}$ is the dispersion profile for the reference atmospheric parameters. The profile shape variation is always less than 0.5 mas, a quantity far smaller than the accuracy of the dispersion model itself. This characteristic allows to compensate the effects of a variation of temperature and pressure just by adjusting the relative rotation of the ADC prisms, provided that the atmospheric dispersion does not exceed the maximum correction achievable with the prisms. For this reason, it is preferable to design the ADC for the atmospheric conditions that cause the maximum dispersion (cold temperatures, high pressures and maximum zenith distance of observation). Another possible approach is to use the standard atmospheric conditions and use a maximum zenith distance slightly bigger than the required one, to accommodate for a variation of the atmospheric parameters.

Table 1. Atmospheric parameters used for the design

PARAMETER	VALUE
Temperature	0.0 °C
Pressure	0.740 atm
Relative humidity	0.125
CO_2 concentration	450 ppm
Maximum zenith distance	65 °
Reference wavelength	633 nm

2.2 ADC design and optimization

In order to match the atmospheric dispersion profile, it is necessary to choose a proper combination of glasses that minimizes the difference between the model and the actual ADC dispersion. To do this, we developed a python code that tries out all the combinations of glasses from an input catalogue and, for each of them, calculates the residual dispersion. As input catalog we used “standard” and “preferred” glasses from Schott, Ohara and Heraeus catalogs, with an internal transmission greater than 98% absolute and 99% average for a 10mm thickness substrate in the wavelength range 370 – 1700nm. This corresponds to a total of ~40 glasses.

The apex angles of the prisms are calculated with a least square optimization algorithm using real ray-tracing equations for the determination of the ADC dispersion as reported in [10]. A similar approach is also used in Pember et al. (2020)^[11]. We adopted an exact ray-tracing approach instead of the typical linear approximation^[10-12] because we found that the accuracy of the latter was not sufficient for the required level of correction (less than ~10mas PTV residuals). As figure of merit for the optimization algorithm, we used the sum of the PTV and RMS residual dispersion defined as:

$$Residuals(\lambda) = \Delta R(\lambda) + 2 \cdot \delta(\lambda) \cdot \frac{D_{pup}}{D_{tel}}$$

Where $\Delta R(\lambda)$ is the atmospheric differential dispersion at $z = 65^\circ$ and with $\lambda_{ref} = 633nm$, $\delta(\lambda)$ is the dispersion (deviation) produced by a single ADC prism. The prism dispersion is multiplied by the pupil de-magnification factor and the factor two accounts for the presence of two prisms. For the optimization, we sampled the dispersion curves with 25 equally spaced wavelengths covering the full wavelength range. Note that, by minimizing the RMS residual dispersion we also minimize the average deviation of the beam exiting the prism, which is one of the required conditions to avoid wobble of the transmitted PSF when rotating the prisms. In fact, when $\lambda = \lambda_{ref}$ the atmospheric differential dispersion $\Delta R = 0$ and the deviation produced by the prism $\delta(\lambda)$ that minimizes the residuals shall be such that $\delta(\lambda_{ref}) \approx 0$.

The results from the python simulations have been validated with the commercial ray-tracing software Zemax OpticStudio, showing almost perfect agreement with the calculated values. In order to simulate atmospheric dispersion in Zemax, we adopted the method suggested by Spanò^[13], approximating the atmosphere with a thin prism by using the gradient5 surface type. Doing this we were able to set a custom dispersion profile based on the Ciddor model instead of using the atmospheric surface model provided by the software that has been demonstrated to underestimate the dispersion at short wavelengths. (see Figure 1).

The python code has been used to optimize the apex angles of the prisms for every glass combination, and to retrieve the residual dispersion. Once the most promising glass combinations were identified, we used Zemax to calculate other relevant optical quantities like total thickness of the prism assembly, transmission and exit pupil shift and to fine-tune the design. In particular, since the exit-pupil stability is relevant for the NGS wavefront sensor sub-module of MAVIS, and is good for calibrations in general, we selected only those combinations for which it was possible to eliminate exit-pupil wobble by adjusting the prism thickness and the angle of incidence on the first face of the prism.

Exit-pupil wobble is generated by any shift of the beam exiting one of the ADC prisms, just like image wobble is generated by any deviation of the beam exiting the ADC. Thus, minimizing exit-pupil wobble means designing a zero-shift Amici prism. This condition can be obtained if the beam shift produced by one glass compensates that produced by the other glasses as shown in Figure 3 for the case of an Amici prism composed by three glasses. In the example reported in figure, the entrance face is orthogonal to the beam. This condition is quite common in ADC design but is not mandatory and, since the total dispersion of the prism is only weakly dependent on the angle of incidence on the first face, especially for small angles of incidence, each prism can be slightly tilted without affecting the overall dispersion behavior. This characteristic is sometimes exploited during alignment to avoid ghost reflections between the entrance and exit face of the ADC, both of them parallel (at least nominally) to the optical axis and placed in a collimated beam, thus generating a focused ghost aligned with the image. During the fine-tuning of the design we used the inclination of the first face as a degree of freedom, together with the thickness of the prisms, to achieve zero beam shift.

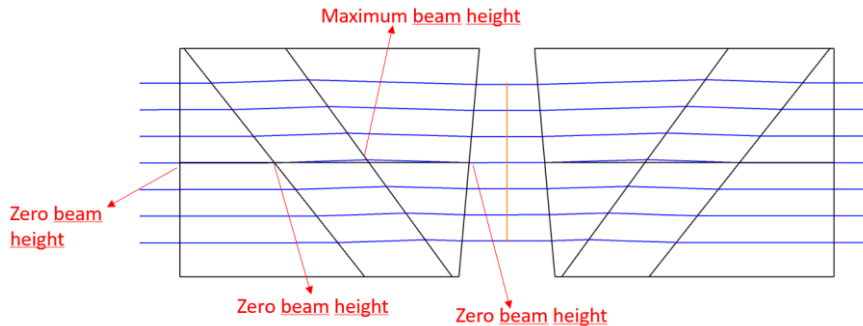


Figure 3. Example of a zero beam-shift ADC

As a first attempt, we searched for combinations of two glasses able to achieve PTV residuals <10mas in the full waveband of the MAVIS common path. The best combination identified in terms of residuals is composed by S-FPL51Y and N-FK58. The first is an i-line (improved transmission in the UV), low dispersion glass from Ohara, the second is an extremely low dispersion glass from Schott. The residual dispersion curve is reported in Figure 4. The nominal PTV residual dispersion is 38mas, with most of the residuals occurring below 500nm.

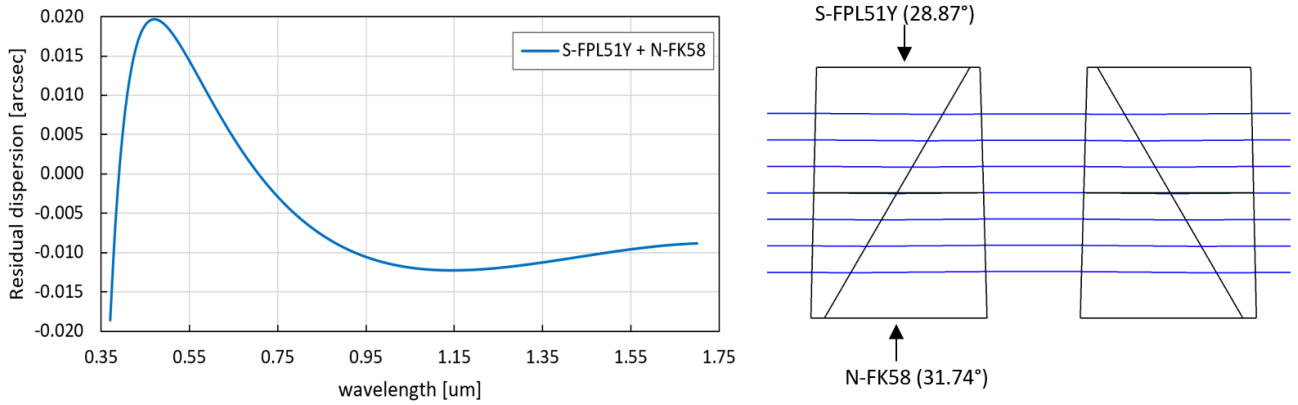


Figure 4. Left: residual dispersion of the S-FPL51Y + N-FK58 ADC. Right: 2D layout of the ADC

Despite the overall good performance of this glass pair, the steep residual dispersion between 370 and 500nm is not optimal and this led us to investigate alternative prism designs formed by three glasses instead of two. The addition of a third glass has a minor impact on the transmission because most of the light is lost due to reflections at air-glass interfaces, whose number is not changed. On the other hand, the added degree of freedom allows to get smaller residuals. This comes at the expense of increased computational time (a few hours in our case to simulate all the ~60.000 combinations) and added complexity in the optimization algorithm. In fact, in the case of three glasses, the convergence is not always well behaved and the optimization algorithm can get stuck on a local minimum. To deal with this issue we used a global optimization algorithm based on the basing hopping method^[14]. The method does not guarantee to find the best minimum for every combination, but it increases the chances to find a global minimum of the merit function. Moreover, running the global optimization algorithm a few times and changing the number of global optimization iterations resulted in almost the same solutions for every run, indicating that a good level of convergence can be achieved with this method.

The most promising glass combinations found by the algorithm are reported in Table 2. In the table we provide the RMS residuals in the visible (370 – 1000nm) and in the near-infrared (1000 – 1700nm), the PTV residuals in the full waveband, the average and minimum transmission in the VIS and NIR regions (accounting for both the ADC prisms and assuming a 2% A/R coating on the air-glass interfaces) and the total center thickness of a single prism assembly. The results are sorted by increasing PTV residual dispersion and all of them can achieve the zero beam-shift condition.

Table 2. Characteristics of the best solutions identified

Glass 1	Glass 2	Glass 3	RMS VIS [mas]	RMS NIR [mas]	PTV [mas]	T_VIS AVG	T_NIR AVG	T_VIS MIN	T_NIR MIN	Thickness [mm]
N-FK58	S-FPL51Y	F2HT	1.0	0.9	4.4	89%	90%	84%	89%	78
S-FPM3	L-LAL15	S-FPL55	1.1	1.3	5.2	84%	86%	72%	84%	70
S-FPL51Y	N-FK58	PBM2Y	0.8	1.5	6.2	88%	89%	84%	88%	78
BAL15Y	N-FK58	S-FPM3	2.0	2.1	7.8	86%	88%	77%	87%	70
N-PK51	PBL26Y	S-FPL55	1.4	3.2	10.8	88%	88%	80%	85%	54
S-FPL51Y	S-FPL53	BAL15Y	4.1	2.1	12.5	89%	89%	85%	88%	73

The first combination has a PTV residual dispersion ~ 8 - 9 times smaller than the 2-glass solution presented above, at the expense of $\sim 1\%$ further loss in transmission and an increase in the thickness of 17mm. The first solution is also the best one in terms of throughput. Note that the first two glasses are the same ones of the 2-glass ADC, with the addition of the F2HT glass, a flint glass from Schott with increased transmission at blue and violet wavelengths.

The other combinations provide an extremely good correction as well, but without clear advantages with respect to the first one except total thickness in the case of N-PK51 + PBL26Y + S-FPL55. However, despite the reduced thickness of almost 25mm, the minimum transmission is $\sim 4\%$ smaller both in the VIS and NIR. For this reason, we adopted the N-FK58 + S-FPL51Y + F2HT combination as the baseline for MAVIS.

Figure 5 shows the residual dispersion curve and the 2D layout of the ADC. The apex angle of the first two prisms is $\sim 35^\circ$, while the third prism is a wedge of about 0.4° . The transmission curve of the ADC is reported in Figure 6 and accounts for Fresnel reflections and bulk absorption of glasses. For every air/glass interface we assumed an ideal and flat A/R coating with 2% reflectivity.

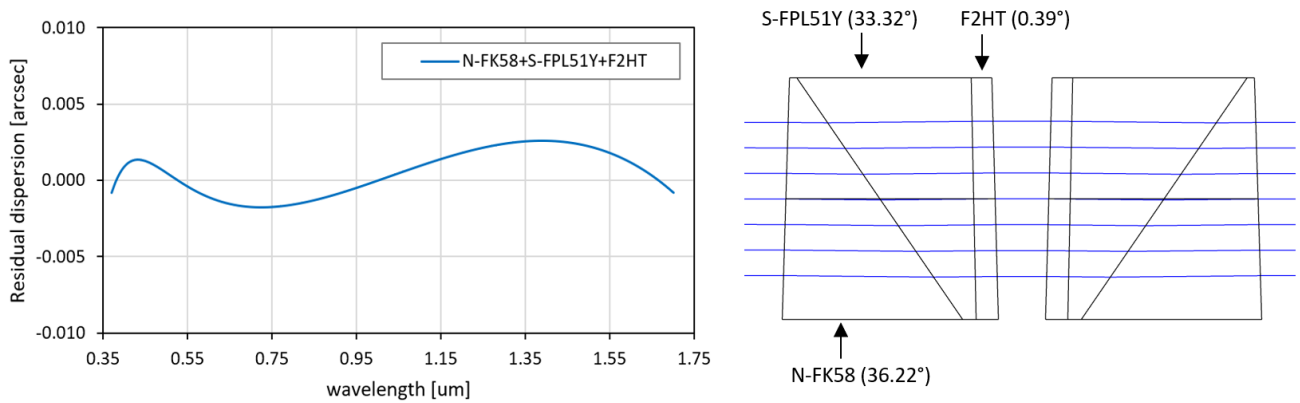


Figure 5. Left: residual dispersion of the N-FK58 + S-FPL51Y + F2HT ADC. Right: 2D layout of the ADC

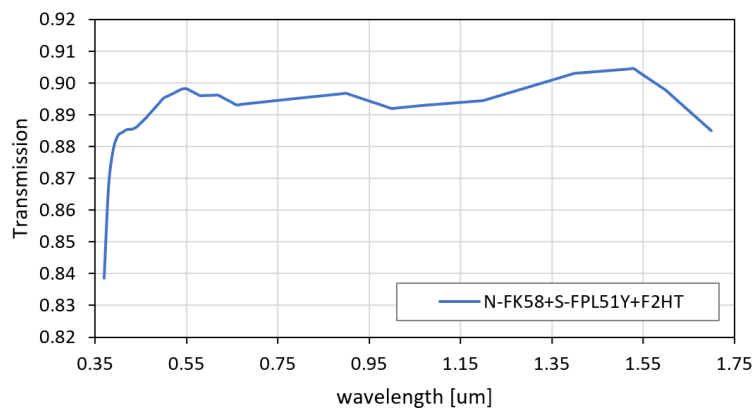


Figure 6. Transmission profile of the N-FK58 + S-FPL51Y + F2HT ADC.

As said before, the exit pupil is affected by a small amount of lateral chromatic aberration due to the fact that the ADC is not in a pupil plane. The total amount of lateral color depends on the tangent of the zenith distance. In the worst condition of $z=65^\circ$ and considering the full wavelength range, the lateral color is equal to $\sim 1\%$ of the pupil diameter. This quantity depends on the distance from the pupil plane, the pupil de-magnification factor and the amplitude of the atmospheric dispersion, while it is almost independent from the design of the prisms.

2.3 Tolerances

Manufacturing tolerances affect both the residual dispersion and the zero-deviation condition. The former can be partially compensated by adjusting the relative rotation of the prisms (only the part of error affecting the amplitude of dispersion and not its “shape”, i.e. any constant multiplicative factor affecting the dispersion curve of one of the prisms). The latter can be compensated by telescope pointing but, doing this, when the prisms are rotated the image will draw a circle in the focal plane. In the case of MAVIS, being the ADC in the common path, any tip-tilt error will be seen by the NGS-WFS and compensated by the AO if the dynamic range is sufficiently high. This allows us to relax the tolerances and avoid image motion in long exposures due to changes in elevation of the telescope.

Even if we do not have yet a complete tolerance analysis for the ADC of MAVIS, it is possible to determine the sensitivity of residual atmospheric dispersion and average deviation due to errors on the dispersion, refractive index and apex angles of the prisms. In order to do this, it is possible to use the linear approximation for the deviation produced by a prism:

$$\Delta(\lambda) = (n(\lambda) - 1) \cdot \alpha$$

Where $\Delta(\lambda)$ is the deviation angle expressed in radians, $n(\lambda)$ is the refractive index of the glass and α is the apex angle of the prism. Here, we consider the following errors:

- Apex angle error: $\delta\alpha$
- Average refractive index error: δn
- Dispersion error: $\delta n(\lambda_{min}) - \delta n(\lambda_{max})$

Introducing these errors in the equation above we can write:

$$\Delta(\lambda)^* = [(n(\lambda) + \delta n + \delta n(\lambda)) - 1] \cdot (\alpha + \delta\alpha)$$

Where the error on the refractive index is expressed as the sum of a wavelength-independent component and a wavelength-dependent component to distinguish between refractive index errors and dispersion errors of the glass. By expanding the equation above for a set of prisms and neglecting second-order terms of error, it can be shown that the variation of the overall dispersion can be expressed as:

$$206265 \frac{D_{pup}}{D_{tel}} \cdot \sum_i \alpha_i \cdot [\delta n_i(\lambda_{min}) - \delta n_i(\lambda_{max})] + \delta\alpha_i [n_i(\lambda_{min}) - n_i(\lambda_{max})] \quad (\text{dispersion error})$$

While the deviation error is given by:

$$206265 \frac{D_{pup}}{D_{tel}} \cdot \sum_i \delta n_i \alpha_i + (n_i - 1) \delta\alpha_i \quad (\text{deviation error})$$

Where the index i denotes different prisms and the errors are in arcsec projected on sky. Considering a reasonable refractive index tolerance of $\delta n = 3 \cdot 10^{-4}$, a dispersion tolerance of $\delta n(\lambda_{min}) - \delta n(\lambda_{max}) = 2 \cdot 10^{-4}$ and an apex error tolerance of $\delta\alpha = 30''$, we get dispersion and deviation errors as high as ~ 100 mas per prism. However, as pointed out before, most of these errors can be compensated. A possible compensation strategy is that of performing precise measurements of the real refractive index of glasses and re-optimizing the apex angles based on the melt data of the blank^[14]. With this strategy, it is possible to reduce by a factor of 10 the errors on refractive index and dispersion. Apex angle errors, on the other hand, can be compensated by adjustment of the clocking angle (for the dispersion error) and telescope pointing/tip-tilt compensation (for the deviation error). The only error that cannot be compensated for is the dispersion profile shape variation of glasses due to melt. A preliminary tolerance analysis based on Montecarlo simulations indicates that, with the re-optimization strategy suggested above, it is possible to keep residual dispersion below ~ 5 -10 mas RMS. These results need to be confirmed considering also other sources of error, but are not in disagreement with what has been found by Wehbe et al. based on real melt data of glasses^[15].

3. CONCLUSIONS

We have presented the optical design of an ultra-broadband atmospheric dispersion corrector for MAVIS covering the wavelength range 370-1700nm. The design is based on counter-rotating Amici prisms that are placed on a collimated beam close to the pupil plane. This is an almost ideal position to avoid the introduction of optical aberrations with the ADC itself. The broad wavelength range and the small number of glasses with high internal transmission from UV to SWIR do not allow to achieve the desired level of correction with a two-glass design. This could have been feasible by allowing a reduced performance below 450nm. We believe that such a solution can be used as a back-up, also considering the fact that AO correction would not give high SR at those wavelengths and at a zenith distance of $z=65^\circ$ (the residuals, like atmospheric refraction, scale as $\tan z$).

Nonetheless, we explored the option of adding a third glass to achieve smaller residual dispersions without impacting too much the throughput of the assembly. In order to do this, we developed a python code able to calculate the angles of the prisms that minimize the residual dispersion with a good convergence towards the minimum of the merit function. The optimization of all the possible glass combinations is quite fast: it takes a few hours on a single core, which is still a reasonable amount of time also to explore different design parameters. In the case of bigger input glass catalogs the simulation time grows quite fast (a couple of days for ~ 100 glasses) and the method can become a bit lengthy, even if not unfeasible in the timeframe of an instrument design.

The results obtained by adding a third glass are very promising, allowing to achieve a factor $\sim 8-9$ decrease of the PTV residuals and giving a broader number of design options. We believe that the same strategy can be applied also to other instruments, especially on 40m-class telescopes, where extremely low levels of residual dispersions are required for some applications like high-resolution imagers and spectrographs^[15]. At the same time, we stress the fact that manufacturing tolerances shall be taken into account as well when considering performance and, below a certain threshold, it is likely that the final performance will be dominated by errors in the refractive index of glasses, the apex angle of the prisms or the alignment of their dispersion axes.

REFERENCES

- [1] Rigaut, F. et al., "MAVIS conceptual design," 11447-332, in these proceedings
- [2] Wynne, C.G., "Correction of atmospheric dispersion in a converging beam", *The Observatory* 104, 140-142 (1984)
- [3] Greggio, D. et al., "MAVIS Adaptive Optics Module optical design", 11448-280, in these proceedings
- [4] Smart W. M., [Textbook on Spherical Astronomy], The University Press, Cambridge (1931)
- [5] Ciddor, P. E., "Refractive index of air: new equations for the visible and near infrared", *Appl. Opt.*, 35, 1566 (1996)
- [6] Filippenko, A. V., "The importance of atmospheric differential refraction in spectrophotometry", *PASP*, 94, 715 (1982)
- [7] Barrell, H., Sears, Junr. J. E., "The refraction and dispersion of air and dispersion of air for the visible spectrum", *Phil. Trans. Roy. Soc. A*, 238 (1939)
- [8] Birch, K. P., Downs, M. J., "An updated Edlén equation for the refractive index of air," *Metrologia*, 30, 155–162 (1993)
- [9] Birch, K. P., Downs, M. J., "Correction to the updated Edlén equation for the refractive index of air," *Metrologia*, 31, 315–316 (1994)
- [10] Hagen, N., Tkaczyk, T. S., "Compound prism design principles, I", *Appl. Opt.*, 50(25), 4998-5011 (2011)
- [11] Pember, J., Schwab, C., Greggio, D., "Selecting optimal glass combinations for atmospheric dispersion correctors", 11451-106, in these proceedings
- [12] Spanò, P., "A super-corrected atmospheric dispersion corrector", *Proc. SPIE*, 7018, 70181G (2008)
- [13] Spanò, P., "Accurate astronomical atmospheric dispersion models in Zemax", *SPIE Proc.*, 9151, 915157 (2014)
- [14] Wales, David J., [Energy Landscapes], Cambridge University Press, Cambridge (2003)
- [15] Wehbe, B., Cabral, A., Ávila, G., "The development of an optical design tool for atmospheric dispersion correction", *SPIE Proc.*, 11207, 112070P (2019)
- [16] Wehbe, B., Cabral, A., Martins, J. H. C., Figueira, P., Santos, N. C., Ávila, G., "The impact of atmospheric dispersion in the performance of high-resolution spectrographs", *Monthly Notices of the Royal Astronomical Society*, 491, 3, 3515–3522 (2020)